Self-Assembly of β-Glucosidase and D-Glucose-Tethering Zeolite Crystals into Fibrous Aggregates

Goo Soo Lee, Yun-Jo Lee, So Yeun Choi, Yong Soo Park, and Kyung Byung Yoon*

Contribution from the Center for Microcrystal Assembly and Department of Chemistry, Sogang University, Seoul 121-742, Korea

Received July 31, 2000

Abstract: β-Glucosidase and D-glucose-tethering micrometer-sized zeolite crystals self-assemble into thin (2−20 μm) and very long (>1 cm) fibrous aggregates in water. The process proceeds at a faster rate in a buffer solution of pH 4.8 at which the enzymatic activity is highest. The zeolite and enzyme remain intact within the fibrous material. Furthermore, the enzymatic activity of β-glucosidase is preserved even after they are kept in water for more than 6 months at room temperature. With the zeolite to enzyme weight ratio of 5, all the zeolite crystals are buried within the round fibrils which consist of either a single strand or helical double strands. Upon increasing the ratio to 10, clusters of unburied zeolite crystals appear on the exterior of the fibrils, while narrow flat fibers with smooth surfaces are formed upon decreasing the ratio to 2.5. The process is proposed to initiate by the tight binding between the zeolite-bound D-glucose moieties and β-glucosidase followed by crystallization of the enzyme over the zeolite-bound enzyme monolayer. This report thus reveals a novel behavior of β-glucosidase and demonstrates an unprecedented phenomenon that an enzyme and its substrate-tethering inorganic crystals self-assemble into structured aggregates.

Introduction

Self-assembly is a process in which atoms, molecules, and systems of molecules arrange themselves into structured functioning entities without human intervention and the most elaborate expression of the process is demonstrated in life systems.[1,2] Studies have shown that self-assembly occurs among numerous substances of all length scales.[1−20] Among these, special attention has been directed to those that involve biologically important interactions such as DNA base pairing and antigen−antibody complexation to gain insights into the natural biological processes.[1−7] However, the enzyme−substrate complexation, which is one of the most important biological interactions, has not yet been explored. In particular, the examples of self-assembly of substances into structured aggregates are very rare.[1−3] Stemming from our interests in organizing zeolite crystals over the surfaces by covalent linkages,[21−26] we have discovered a novel phenomenon that β-glucosidase and the D-glucose-tethering zeolite crystals readily self-assemble into thin and long fibrous aggregates. Interestingly, the enzymatic activity of β-glucosidase in the fibrous composite material is preserved even after they were stored in water for 6 months at room temperature. This paper reports the unprecedented, highly intriguing phenomenon of self-assembly of an enzyme and its substrate-tethering micrometer-sized inorganic crystals into structured entities.

Experimental Section

Materials. β-Glucosidase (lot number 37H0947, recombinant) and *p*-nitrophenyl β-D-glucopyranoside (PNPG) were purchased from Sigma. D-Glucose, D-cellobiose, ω-undecylenyl bromide, 4-hydroxy-

(1) Whitesides, G. M. *Sci. Am.* **1995**, *273*, 146−149.
(2) Ozin, G. A. *Chem. Commun.* **2000**, 419−432.
(3) Boal, A. K.; Ilhan, F.; DeRouchey, J. E.; Thurn-Albrecht, T.; Russell, T. P.; Rotello, V. M. *Nature* **2000**, *404*, 746−748.
(4) Shenton, W.; Davis, S. A.; Mann, S. *Adv. Mater.* **1999**, *11*, 449−451.
(5) Li, M.; Wong, K. K. W.; Mann, S. *Chem. Mater.* **1999**, *11*, 23−26.
(6) Alivisatos, A. P.; Johnsson, K. P.; Peng, X.; Wilson, T. E.; Loweth, C. J.; Bruchez, M. P., Jr.; Schultz, P. G. *Nature* **1996**, *382*, 609−611.
(7) (a) Taton, T. A.; Mucic, R. C.; Mirkin, C. A.; Letsinger, R. L. *J. Am. Chem. Soc*. **2000**, *122*, 6305−6306. (b) Storhoff, J. J.; Mirkin, C. A. *Chem. Rev.* **1999**, *99*, 1849−1862. (c) Mirkin, C. A.; Letsinger, R. L.; Mucic, R. C.; Storhoff, J. J. *Nature* **1996**, *382*, 607−609. (d) Elghanian, R.; Storhoff, J. J.; Mucic, R. C.; Letsinger, R. L.; Mirkin, C. A. *Science* **1997**, *277*, 1078−1081.
(8) Li, M.; Schnablegger, H.; Mann, S. *Nature* **1999**, *402*, 393−395.
(9) Murray, C. B.; Kagan, C. R.; Bawendi, M. G. *Science* **1995**, *270*, 1335−1338.
(10) Andres, R. P.; Bielefeld, J. D.; Henderson, J. I.; Janes, D. B.; Kolagunta, V. R.; Kubiak, C. P.; Mahoney, W. J.; Osifchin, R. G. *Science* **1996**, *273*, 1690−1693.
(11) Sun, S.; Murray, C. B.; Weller, D.; Folks, L.; Moser, A. *Science* **2000**, *287*, 1989−1992.
(12) Stupp, S. I.; LeBonheur, V.; Walker, K.; Li, L. S.; Huggins, K. E.; Keser, M.; Amstutz, A. *Science* **1997**, *276*, 384−389.
(13) Petit, C.; Taleb, A.; Pileni, M.-P. *Adv. Mater.* **1998**, *10*, 259−262.
(14) Motte, L.; Billoudet, F.; Lacaze, E.; Pileni, M.-P. *Adv. Mater.* **1996**, *8*, 1018−1020.
(15) Brust, M.; Bethell, D.; Schiffrin, D. J.; Kiely, C. J. *Adv. Mater.* **1995**, *7*, 795−797.
(16) Wang, Z. L. *Adv. Mater.* **1998**, *10*, 13−30.
(17) Bowden, N.; Terfort, A.; Carbeck, J.; Whitesides, G. M. *Science* **1997**, *276*, 233−235.
(18) Weck, M.; Choi, I. S.; Jeon, N. L.; Whitesides, G. M. *J. Am. Chem. Soc.* **2000**, *122*, 3546−3547.
(19) Bowden, N.; Choi, I. S.; Grzybowski, B. A.; Whitesides, G. M. *J. Am. Chem. Soc.* **1999**, *121*, 5373−5391.
(20) Choi, I. S.; Bowden, N.; Whitesides, G. M. *J. Am. Chem. Soc.* **1999**, *121*, 1754−1755.
(21) Kulak, A.; Lee, Y.-J.; Park, Y. S.; Yoon, K. B. *Angew. Chem., Int. Ed.* **2000**, *39*, 950−953.
(22) Choi, S. Y.; Lee, Y.-J.; Park, Y. S.; Ha, K.; Yoon, K. B. *J. Am. Chem. Soc.* **2000**, *122*, 5201−5209.
(23) Ha, K.; Lee, Y.-J.; Lee, H. J.; Yoon, K. B. *Adv. Mater*. **2000**, *12*, 1114−1117.
(24) Lee, G. S.; Lee, Y.-J.; Ha, K.; Yoon, K. B. *Tetrahedron* **2000**, *56*, 6965−6968.
(25) Ha, K.; Lee, Y.-J.; Jung, D.-Y.; Lee, J. H.; Yoon, K. B. *Adv. Mater*. **2000**, *12*, 1614−1617.
(26) Kulak, A.; Park, Y. S.; Lee, Y.-J.; Chun, Y. S.; Ha, K.; Yoon, K. B. *J. Am. Chem. Soc*. **2000**, *122*, 9308−9309.

10.1021/ja0028222 CCC: $19.00
Published on Web 11/22/2000

Scheme 1

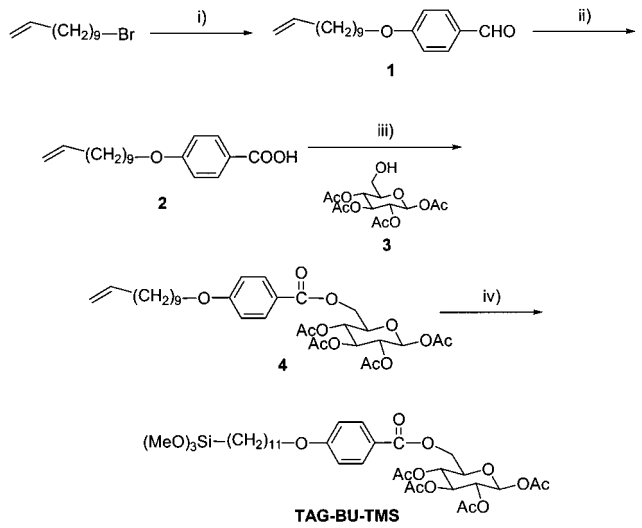

benzaldehyde, sodium chlorite, and hydrogen hexachloroplatinate were purchased from Aldrich and were used as received. Trimethoxysilane (Aldrich) was distilled and kept in a Schlenk storage flask under argon. All the organic solvents were purified according to the well-known literature procedures prior to use. Reflectoquant, a qualitative test strip for D-glucose, was purchased from Merck. A buffer solution of pH 4.8 was prepared from a 1:1 mixture of acetic acid (0.01 M) and sodium acetate (0.01 M).

Zeolite-A (Na^+ form) and ZSM-5 (Si/Al = 100) were synthesized according to the literature procedures.[27] The average size of zeolite-A used in this study was ~0.4 μm and that of ZSM-5 was ~1.5 × 1.1 × 0.6 μm^3. The template ions such as tetramethylammonium (TMA^+) and tetrapropylammonium (TPA^+) employed during synthesis of zeolite-A and ZSM-5, respectively, were removed by calcining at 550 °C for 12 h under flowing oxygen prior to treatment of the zeolite crystals with the following silylating reagent (vide infra).

Preparation of 1,2,3,4-Tetra-*O*-acetyl-6-*O*-{4-[11-(trimethoxysilyl)undecyloxy]benzoyl}-β-D-glucose (TAG-BU-TMS). As a means to tether D-glucose to zeolite crystals, TAG-BU-TMS was prepared according to Scheme 1 as described in detail in the following steps.

Preparation of 4-(10-Undecenyloxy)benzaldehyde (1). 11-Bromo-1-undecene (2.19 mL, 2.33 g, 10 mmol), 4-hydroxybenzaldehyde (1.22 g, 10 mmol), tetrabutylammonium iodide (catalytic amount, 0.10 g), and potassium carbonate (6.90 g, 50 mmol) were introduced into acetone (50 mL). After refluxing for 6 h, the mixture was allowed to cool to room temperature and the solids were filtered off. The filtrate was concentrated in vacuo and the crude product of **1** was purified by column chromatography (ethyl acetate:hexane = 1:4). $C_{18}H_{26}O_2$ 274.40, yield 2.33 g (85%), colorless oil, ^{1}H NMR ($CDCl_3$, δ/ppm) 9.87 (s, 1H), 7.82 (d, 2H), 6.98 (d, 2H), 5.80 (m, 1H), 4.96 (m, 2H), 4.03 (t, 2H), 2.03 (m, 2H), 1.81 (m, 2H), 1.31−1.48 (12H).

Preparation of 4-(10-Undecenyloxy)benzoic Acid (2). The aldehyde **1** (2.00 g, 7.29 mmol) and resorcinol (1.05 g, 9.50 mmol) were dissolved in *tert*-butyl alcohol (140 mL). Independently, sodium chlorite (3.80 g) and sodium dihydrogenphosphate (3.04 g) were dissolved in water (30 mL). The aqueous solution was added in a dropwise manner into the *tert*-butyl alcohol solution over a 10-min period. The pale yellow reaction mixture was then stirred at room temperature overnight. Volatile components were removed in vacuo and the residue was dissolved in water (100 mL). The aqueous solution was acidified to pH 3 by adding 1 N aqueous HCl. The liberated white precipitate was isolated, washed successively with water and hexane, and dried in the air. $C_{18}H_{26}O_3$ 290.40, yield 1.97 g (93%), white solid, mp 79.5−80 °C, ^{1}H NMR ($CDCl_3$, δ/ppm) 8.05 (d, 2H), 6.92 (d, 2H), 5.80 (m, 1H), 4.96 (m, 2H), 4.02 (t, 2H), 2.05 (m, 2H), 1.81 (m, 2H), 1.31−1.46 (12H).

(27) (a) Zhu, G.; Qui, S.; Yu, J.; Sakamoto, Y.; Xiao, F.; Xu, R.; Terasaki, O. *Chem. Mater*. **1998**, *10*, 1483−1486. (b) U.S. Patent 3702886, 1972. (c) U.S. Patent 4061724, 1977.

Preparation of 1,2,3,4-Tetra-*O*-acetyl-β-D-glucose (TAG, 3). Anhydrous α-D-glucose (12.0 g, 67 mmol) and triphenylmethyl chloride (19.3 g 69 mmol) were dissolved in anhydrous pyridine (50 mL) by warming on a steam bath. The yields depend on the dryness of the reagents and containers. Acetic anhydride (30 mL) was poured in one portion into the pyridine solution without cooling. The solution was allowed to cool to room temperature and kept at that temperature for an additional 12 h. The above mixture was then introduced in a thin stream into the mixture of ice water (950 mL) and acetic acid (50 mL) while rapidly swirling the container. After 2 h of vigorous agitation the precipitate was isolated by filtration. To remove residual pyridine, the gummy filter cake was immediately introduced into fresh ice water (1 L) and the mixture was stirred for an additional 10 min. White precipitate was isolated by filtration and subsequently washed with copious amounts of fresh water. As a means to preferentially remove the α-isomer, which has higher solubility in diethyl ether, the crude, air-dried product was then introduced into diethyl ether (50 mL). The less soluble β-isomer was isolated and recrystallized from hot 95% ethanol. Upon cooling, fine needle forms of crystalline 1,2,3,4-tetra-*O*-acetyl-6-*O*-triphenylmethyl-β-D-glucose were liberated. $C_{33}H_{34}O_{10}$ 590.62, yield 17 g (43%), mp 166−167 °C. The above tritylated compound (7.4 g, 12.5 mmol) was dissolved in glacial acetic acid (35 mL) by warming on a water bath. The solution was cooled to 10 °C, then the glacial acetic acid solution of hydrogen bromide (33%, 2.7 mL) was added and the mixture was shaken for 45 s. The liberated triphenylmethyl bromide was immediately removed by suction filtration, and the filtrate was poured in one portion into ice water (150 mL). The produced glucose tetraacetate (TAG) was extracted with chloroform (4 × 40 mL). The extract was washed with cold water (15 mL × 4) to remove residual acetic acid and then dried over anhydrous magnesium sulfate. The solvent in the extract was stripped off in vacuo. Anhydrous diethyl ether (15 mL) was introduced onto the syrupy residue. Crystallization began immediately upon rubbing the syrup using a glass rod. The compound slowly decomposes above −10 °C. $C_{14}H_{20}O_{10}$ 348.30, yield 3.4 g (78%), white solid, mp 128−129 °C, ^{1}H NMR ($CDCl_3$, δ/ppm) 5.74 (d, 1H), 5.32 (t, 1H), 5.10 (m, 2H), 3.77 (m, 1H), 3.57−3.69 (m, 2H), 2.12 (s, 3H), 2.08 (s, 3H), 2.05 (s, 3H), 2.04 (s, 3H).

Preparation of 1,2,3,4-Tetra-*O*-acetyl-6-*O*-[4-(10-undecenyloxy)-benzoyl]-β-D-glucose (4). The acid **2** (1.91 g, 6.6 mmol), TAG **3** (2.30 g, 6.6 mmol), dicyclohexylcarbodiimide (DCC, 2.72 g, 13.2 mmol), and 4-(*N*,*N*-dimethylamino)pyridine (DMAP, 0.40 g, 3.30 mmol) were dissolved in dichloromethane (60 mL), and the solution was stirred at room temperature for 3 h. Acetic acid (5 mL) and methanol (5 mL) were successively added into the mixture to destroy the excess DCC. The mixture was additionally stirred at 45 °C for 30 min. After cooling to room temperature, the mixture was filtered through a silica pad. The filtrate was concentrated in vacuo and the crude product was purified by column chromatography (ethyl acetate:hexane = 1:4). The product was further purified by recrystallization from methanol. $C_{32}H_{44}O_{12}$ 620.69, yield (2.59 g, 63%), white solid, mp 99.5−100 °C, ^{1}H NMR ($CDCl_3$, δ/ppm) 7.99 (d, 2H), 6.91 (d, 2H), 5.84 (m, 1H), 5.77 (d, 1H), 5.13−5.33 (m, 3H), 4.95 (m, 2H), 4.32−4.49 (m, 2H), 4.01 (t, 2H), 3.98 (m, 1H), 2.09 (s, 3H), 2.02 (s, 3H), 2.00 (s, 6H), 1.78 (m, 2H), 1.30−1.44 (14H). ^{13}C NMR ($CDCl_3$, δ/ppm) 169.99, 169.21, 169.17, 168.80, 165.75, 163.20, 139.11, 131.79, 121.58, 114.13, 114.06, 91.71, 72.87, 72.78, 70.31, 68.16, 61.86, 33.71, 29.40, 29.32, 29.25, 29.02, 28.84, 25.90, 20.70, 20.48.

Preparation of TAG-BU-TMS. Anhydrous toluene (5 mL) was introduced into a round-bottomed flask containing the olefin **4** (620 mg, 1 mmol) and hydrogen hexachloroplatinate (catalytic amount, ~0.1 mg) under argon. Trimethoxysilane (0.3 mL, 293 mg, 2.4 mmol) was introduced into the mixture using a hypodermic syringe and the mixture was stirred at 42 °C for 15 h. After cooling to room temperature, the mixture was immediately filtered through double pads of silica and charcoal by applying argon pressure. Upon concentrating the filtrate, TAG-BU-TMS was obtained as an extremely hygroscopic solid. $C_{35}H_{54}O_{15}Si$ 742.88, quantitative yield, ^{1}H NMR ($CDCl_3$, δ/ppm) 7.98 (d, 2H), 6.91 (d, 2H), 5.75 (d, 1H), 5.13−5.33 (m, 3H), 4.33−4.48 (m, 2H), 4.00 (t, 2H), 3.97 (m, 1H), 3.56 (s, 9H), 2.10 (s, 3H), 2.03 (s, 3H), 2.01 (s, 6H), 1.79 (m, 2H), 1.28−1.42 (14H). ^{13}C NMR ($CDCl_3$,

Scheme 2

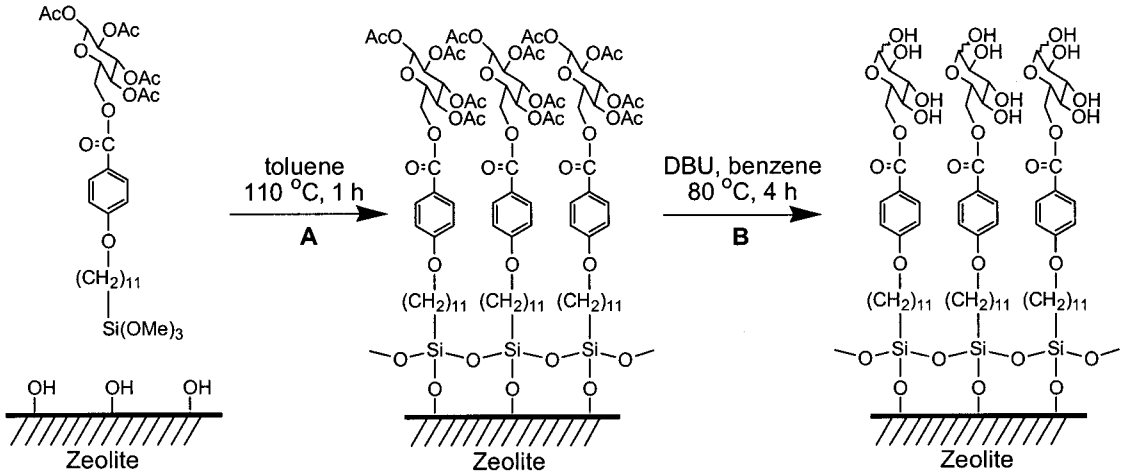

δ/ppm) 170.07, 169.28, 169.24, 168.88, 165.83, 163.28, 131.85, 121.62, 114.19, 114.06, 91.78, 72.93, 72.84, 70.36, 68.23, 61.93, 50.45, 33.10, 29.56, 29.52, 29.47, 29.35, 29.22, 29.10, 25.97, 22.58, 20.76, 20.53, 20.52, 9.15.

Attachment of TAG Groups on Zeolite Surface (Step A in Scheme 2**).** Dry toluene (50 mL) was introduced into a round-bottomed Schlenk flask containing freshly dried zeolite-A (100 mg) or ZSM-5 (100 mg) under a counter flow of argon. The toluene slurry was sonicated for 10 min to disperse the zeolite crystals into the solution. Independently, dry toluene (10 mL) was introduced into a round-bottomed Schlenk flask containing TAG-BU-TMS (150 mg) under an argon flow. The TAG-BU-TMS solution was transferred to the sonicated toluene slurry under argon. The mixture was refluxed for 1 h under argon atmosphere. After cooling to room temperature, the TAG-BU-tethering zeolite powders were collected by rapid filtration in the atmosphere over a filter paper. The filtered powders were washed successively with fresh toluene (100 mL) and ethanol (100 mL). The collected powders were dried in an oven at 120 °C for 30 min.

Deacetylation of TAG Groups Tethered to Zeolite Crystals. Dry benzene (100 mL) was introduced into a round-bottomed Schlenk flask containing the TAG-tethering zeolite-A or ZSM-5 (100 mg) under argon. 1,8-Diazabicyclo[5.4.0]undec-7-ene (DBU, 0.3 mL), a reagent known to selectively cleave the acetyl groups from glucose,[28] was added to the zeolite slurry in benzene and the mixture was refluxed for 4 h under argon. After cooling to room temperature, the glucose-coated zeolite powders were collected by rapid filtration in the atmosphere over a filter paper. The filtered powders were washed successively with fresh toluene (100 mL) and ethanol (100 mL). The collected powders were dried in an oven at 120 °C for 30 min (step B in Scheme 2).

Formation of Fibrous Zeolite-β-Glucosidase Composite Material. β-Glucosidase (2 mg) was introduced into distilled deionized water (20 mL) dispersed with TAG-tethering zeolite-A (10 mg). The slurry was stirred with the aid of a small magnetic stirrer at room temperature. A Teflon slab with four supporting legs was introduced into the reaction vessel to collect the precipitating fibrous aggregates upon it. The added amounts of enzyme were also varied from 2 to 1 and 4 mg to see the effect of the zeolite/enzyme weight ratio. The fibrillation was also tested in an acetate buffer solution of pH 4.8 to check the effect of the pH, at which the enzymatic activity of β-glucosidase is known to be highest, on the rate of fibrillation.

Test of Enzymatic Activity of Fibrous Composite Fiber. The composite fiber (1 mg) and D-cellobiose (10 mg) were introduced into water (10 mL) and the heterogeneous mixture was allowed to equilibrate for 24 h. A strip of Reflectoquant was dipped into the solution for 10 s. After removal from the solution, the strip was dried for a visual color test. Alternatively, the composite fiber (1 mg) was added into 1 mL of the citrate−phosphate buffer solution (100 mM, pH 5) dissolved with PNPG (15 mM).[29] The fibril-induced hydrolysis of PNPG was allowed to proceed for 30 min at 30 °C. A $Na_2CO_3/NaHCO_3$ buffer solution (5 mL, 50 mM, pH = 10.2) was subsequently introduced into the PNPG solution to quench the activity of the enzyme. The released *p*-nitrophenol was monitored spectrophotometrically at 400 nm using the molar extinction coefficient of 14 130 $M^{-1}cm^{-1}$.[29] For the long-term activity tests, the composite fibers were stored in fresh water and the activity was occasionally tested by employing the more convenient Reflectoquant strips. Since the composite fiber is highly fluffy, the volume of even 1 mg was large enough to weigh accurately using a microbalance.

Instrumentation. The scanning electron microscope (SEM) images of zeolites, crystalline β-glucosidase, and the zeolite-β-glucosidase composite fibers were obtained from a FE-SEM (Hitachi S-4300) at an acceleration voltage of 10 to 20 kV. On top of the samples platinum/palladium alloy (in the ratio of 8 to 2) was deposited with a thickness of about 15 nm. The X-ray diffraction patterns for the identification of the zeolite crystals were obtained from a Rigaku diffractometer (D/MAX-1C) with the monochromated beam of Cu Kα. The UV−vis spectra of the samples were recorded on a Shimadzu UV-3101PC. The diffuse reflectance UV−vis spectra of solid samples were obtained using an integrating sphere. FT-IR spectra were recorded on a JASCO FT/IR-620. The solution ^1H and ^{13}C NMR spectra were recorded on a Varian Jemini 300 NMR spectrometer. ^{13}C, ^{27}Al, and ^{29}Si MAS solid-state NMR spectra were recorded on a Varian 300 Unity Inova NMR spectrometer. Freeze-drying of the fibrous composite materials was conducted on a LABCONCO Freezone 6.

Results and Discussion

I. Confirmation of D-Glucose Tethered to Zeolite Crystals. The ready attachment of TAG via the BU-SiO spacer to the zeolite crystals was confirmed by the close matching between the intense diffuse-reflectance UV−vis band of the TAG-BU-TMS-treated zeolite crystals centered at 260 nm (Figure 1) and the corresponding absorption of TAG-BU-TMS in ethanol at 259 nm (shown in the inset), due to the presence of a phenyl moiety in both cases. The appearance of a carbonyl stretching band at 1762 cm^{-1} in the diffuse-reflectance FT-IR spectrum of the zeolite crystals treated with TAG-BU-TMS further confirmed the ready attachment of TAG groups to the zeolite crystals via siloxane linkages. Consistent with this, the TAG-tethering zeolite crystals became very hydrophobic and consequently floated on water.

Restoration of hydroxyl groups on the glucose units was first confirmed by the appearance of broad multiple hydroxyl stretching bands in the 3000−3600 cm^{-1} region of the diffuse-

(28) Baptistella, L. H. B.; Santos, J. F.; Ballabio, K. C.; Marsaioli, A. J. *Synthesis* **1989**, 436−438.

(29) Riccio, P.; Rossano, R.; Vinella, M.; Domizio, P.; Zito, F.; Sansevrino, F.; D'Elia, A.; Rosi, I. *Enzyme Microb. Technol.* **1999**, *24*, 123−129.

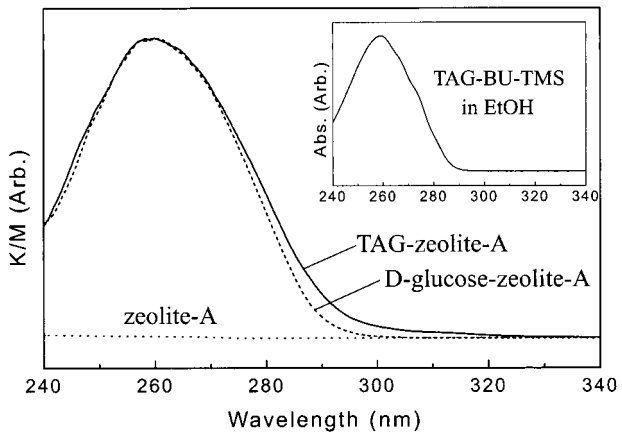

Figure 1. Diffuse-reflectance UV−vis spectra of zeolite-A tethered with TAG (—), D-glucose (- - -), and none (•••). The inset shows the spectrum of TAG-BU-TMS in ethanol.

reflectance FT-IR spectrum of the DBU-treated zeolite powders (Figure 2C). The BU-SiO spacer being intact after treatment with DBU was confirmed from the presence of the 260-nm band (due to the phenyl moiety) in the diffuse reflectance UV−vis spectrum (dashed curve in Figure 1). The positive periodate test for vicinal diols and the Benedict's test for formyl groups further confirmed the presence of glucose units on the surface. Consistent with the restoration of hydroxyl groups, the DBU-treated zeolite powders turned hydrophilic and as a result they readily dispersed into water.

II. Formation of Fibrous Zeolite-β-Glucosidase Composite Material. The aqueous slurry of D-glucose-tethering zeolite-A powders remained turbid for an unlimited period of time as long as the solution was kept stirred. Upon addition of β-glucosidase, however, the turbid solution gradually turned clear while a fibrous material slowly developed in the solution, in particular, over the immersed Teflon support. After 2 days of stirring, the solution turned completely transparent and the produced fibrous material became visually apparent as shown in Figure 3.

The presence of Teflon support was not necessary for the above fibrillation to occur. However, it helped the fibrils grow into a larger aggregate without being chopped into smaller fragments by the underlying spinning magnetic bar. Even the magnetic stirring bar was not necessary for the fibrillation to proceed. Any methods to maintain dispersion of the micro zeolite crystals into the solution are equally effective. The nature of the container (glass or plastic) also did not affect the fibrillation process and the fibrils did not grow on the walls of the containers, indicating that the container walls do not serve as the seeds or anchoring spots for the fibrils to grow. The density of the resulting fibrils was apparently larger than that of water hence readily submerged onto the bottom of the containers.

The fibrillation process proceeded at a much faster rate in an acetate buffer solution of pH 4.8. Thus, while it took 48 h in distilled deionized water, only 8 h was enough to complete the fiber-forming process in the buffer solution. This indicates an about 6-fold increase in the rate. Considering the fact that the activity of β-glucosidase is highest at pH 4.8,[30] this result indicates that the enzymatic activity plays a crucial role in the fibrillation.

In strong contrast, the fiber-forming process did not proceed at all even after much longer periods of stirring (>1 month) if the acetyl groups are not removed from the TAG units nor if plain (TAG-free) zeolite-A crystals are employed. This result suggests that the presence of D-glucose units on the zeolite surfaces is essential for the structure-forming process. Thermal denaturation of the enzyme[31] induced by boiling the aqueous solution of the enzyme for 2 h prior to introduction to the aqueous slurry of D-glucose-tethering zeolite-A also did not lead to fibrillation. Chemical denaturation of the enzyme induced by addition of sodium dodecyl sulfate (50 mg per 2 mg of enzyme), a well-known chemical denaturant,[32] into the mixture also effectively prevented fibrillation. These results underscore that the preservation of the enzyme in its originally active state is essential for the fibrillation.

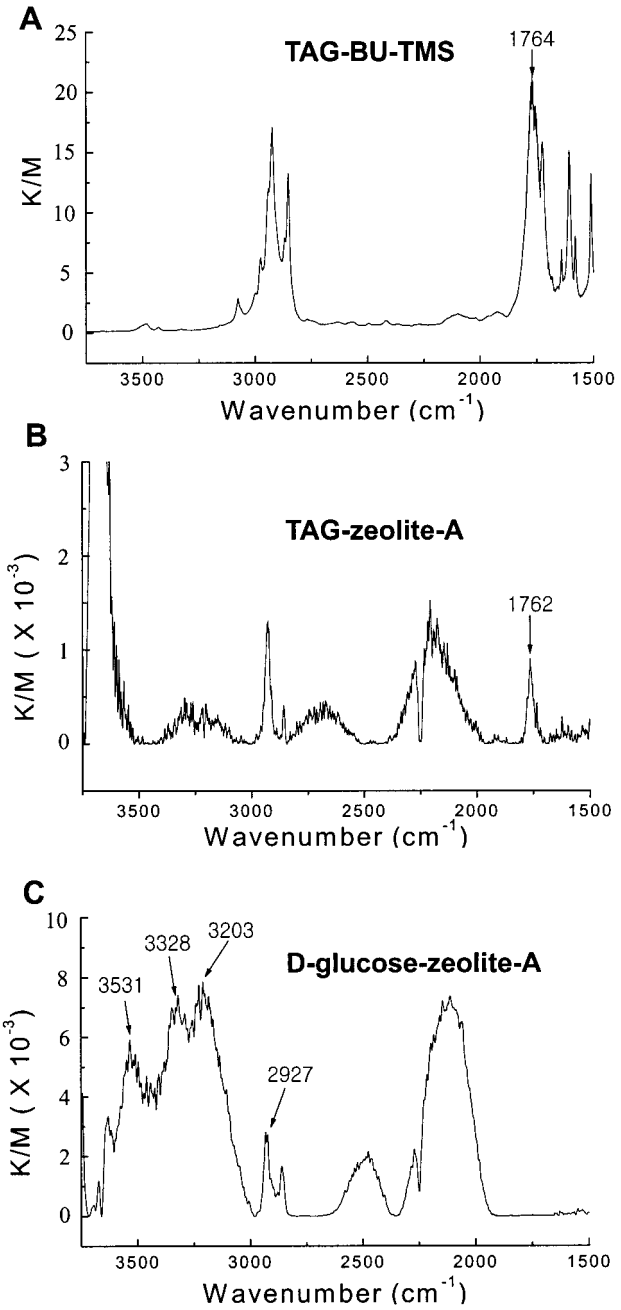

Figure 2. Diffuse-reflectance FT-IR spectra of solid TAG-BU-TMS (A) and the zeolite crystals tethering TAG (B) and D-glucose (C) units, respectively, via BU-SiO spacers.

(30) Tanaka, T.; Oi, S. *Agric. Biol. Chem.* **1985**, *49*, 1267−1273.

(31) Wong, C.-H.; Whitesides, G. M. *Enzymes in Synthetic Organic Chemistry*; Pergamon Press: 1994; pp 17−18.

(32) Boyer, R. *Concepts in Biochemistry*; Brooks/Cole: London, 1999; pp 125−126.

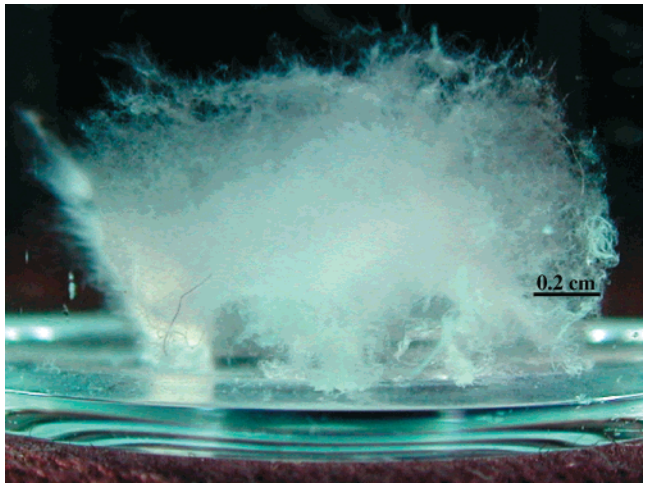

Figure 3. A photographic image showing the fibrous nature of the zeolite-A-β-glucosidase composite material.

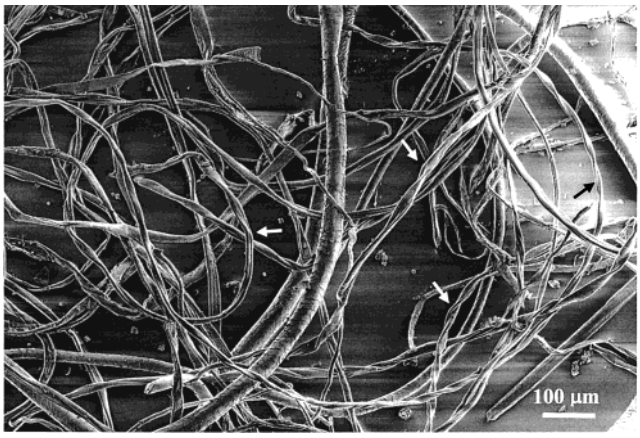

Figure 4. A typical SEM image showing the fibrous zeolite-A-β-glucosidase composite material obtained from an aqueous mixture of D-glucose-tethering zeolite-A and the enzyme in the weight ratio of 5.

It should also be noted that the highly water soluble β-glucosidase alone, either in the presence or absence of a large amount (100 mM) of plain, unmodified D-glucose, does not spontaneously crystallize into such fibrils as long as the glucose-tethering zeolite-A crystals is left out. On the basis of the above facts, we propose that the enzyme−substrate interaction between β-glucosidase and D-glucose units tethered to zeolite surface is essential for the above fibrillation to occur. In strong support to this, the fibrillation of β-glucosidase and D-glucose-tethering zeolite crystals did not proceed in a highly concentrated (100 mM) solution of D-glucose, due to the inhibiting effect of free D-glucose molecules on the fibrillation.

III. Morphology of the Fibrous Composite. The scanning electron microscope (SEM) images of the freeze-dried fibrous material clearly showed the fibrous morphology of the aggregated material as typically shown in Figure 4. The cross-sectional diameters of the cylindrical fibers range from 2 to 20 μm but more commonly from 5 to 15 μm. The closer looks of the terminals of the thick cylindrical fibers revealed that they split into several thinner fibers. As indicated by arrows in Figure 4, many fibers also exist in the helical forms as two strands twisted together. The lengths of some of intermingled fibers even exceed a few centimeters. The fibers resumed growing upon addition of fresh D-glucose-tethering zeolite-A crystals and β-glucosidase into the transparent solution containing the fibrils.

Interestingly, the presence of zeolite crystals within the fibers was not apparent from the SEM images. However, the cross-sectional view of SEM images of the cylindrical fibers revealed that they consist of lumps that look like zeolite-A crystals covered with thick enzyme layers as typically shown in Figure 5. The presence of zeolite-A crystals within the fibrils was apparent from the identical magic angle spinning solid-state ^{27}Al and ^{29}Si NMR spectra of the fibrils and the plain, unmodified zeolite-A crystals (Figure 6, panels A and B). The fact that the cubic morphology of zeolite-A crystals remains intact within the fibrous composite was apparent from the SEM image of the remained zeolite crystals after heating the composite fibers at 520 °C under flowing oxygen to burn off the organic enzyme (Figure 7). The presence of β-glucosidase as the single organic species within the fibrous material was also confirmed from the two identical solid-state ^{13}C NMR spectra of the neat enzyme and the composite fiber (Figure 6C). The above results hence clearly verify that the fibrils consist of only zeolite-A crystals and β-glucosidase and the zeolite crystals are buried within the fibrils. A similar fibrous material also readily developed from the aqueous mixture of β-glucosidase and the larger, prismatic ZSM-5 crystals tethered with D-glucose, indicating that the morphology of the inorganic crystal does not affect that of the fiber.

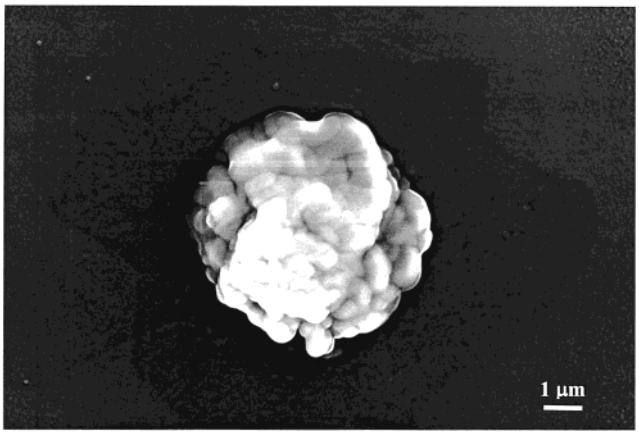

Figure 5. A typical SEM image of the cross section of a cylindrical zeolite-A-β-glucosidase fibrous material showing the lumpy enzyme-coated zeolite-A crystals.

Upon increasing the zeolite to β-glucosidase weight ratio to 10, unburied clusters of zeolite-A crystals appeared on the exterior of most of the fibrils (Figure 8, panels A and B). Upon decreasing the ratio to 2.5, all the zeolite crystals were again buried within the fibers but the fibers became flat narrow bands resembling the flakelike morphology of the crystalline enzyme (Figure 9). This result showed that the zeolite to enzyme weight ratio sensitively affects the cross-sectional shape of the fibrous aggregates.

IV. Insights into the Mechanism of the Fibrillation. To gain insight into the fibrillation process, a few drops of the aqueous slurries were periodically taken out of reaction vessels at early and intermediate stages of the fibrillation process and freeze-dried for SEM analyses. As shown in Figure 10A, it was found that crystalline β-glucosidase starts surrounding the zeolite-A crystals. The material that surrounds zeolite crystals being crystalline β-glucosidase was obvious not only from the spectrum of solid-state ^{13}C NMR but also from the fact that the flat morphology of the surrounding material resembles that of β-glucosidase shown in Figure 9. It was also revealed that the enzyme binds several zeolite crystals into randomly aggregated clusters by crystallizing between the zeolite crystals (Figure 10B). Some of SEM images also revealed that the randomly aggregated zeolite clusters are further interwoven by intercon-

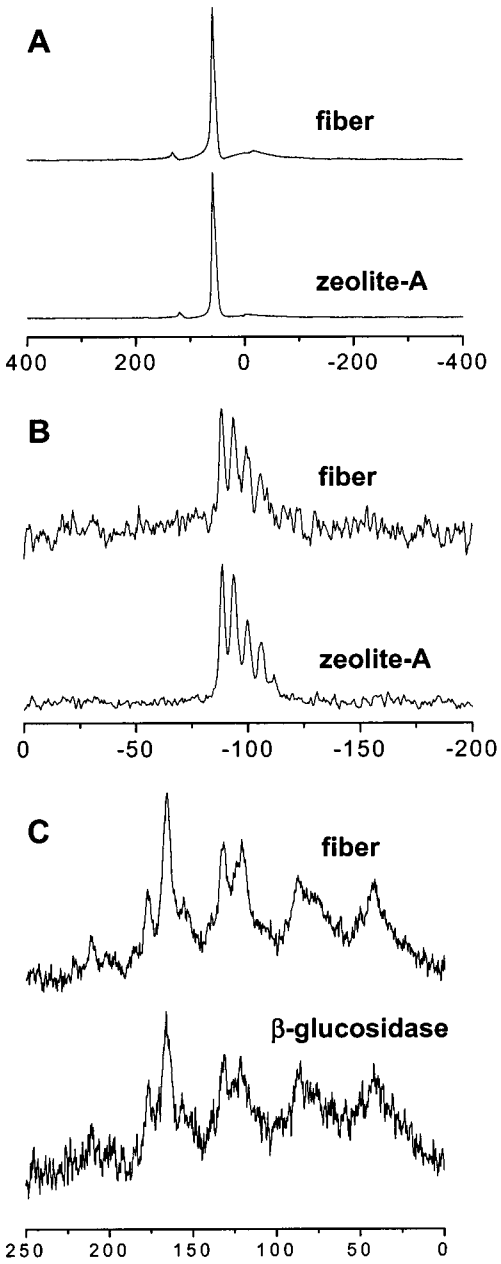

Figure 6. MAS solid-state NMR spectra of the fibrous zeolite-A-β-glucosidase composite material and its corresponding reference material (as indicated): ^{27}Al (A), ^{29}Si (B), and ^{13}C (C).

necting crystalline β-glucosidase crystallites (Figure 10C). In strong contrast, phase separation of the turbid mixture into piles of zeolite crystals and the crystalline enzyme results as shown in Figure 10D if the zeolite crystals are not tethered with D-glucose. This result indicates that drying artifact is not the reason for the observed intermediate stages of fibrillation (panels A, B, and C).

Based on the facts presented so far, we propose that the fibrillation occurs according to Scheme 3. First, β-glucosidase binds to each D-glucose unit tethered to zeolite crystals via enzyme−substrate complexation (step A). The surface-covering monolayers of enzymes then act as pseudocrystalline surfaces that in turn serve as seed surfaces for the enzymes to start crystallizing over the surfaces (step B). At the present moment, however, the question about the nature of the driving force to attract such a highly water-soluble enzyme from the aqueous solution onto the substrate-tethering surface remains open. The zeolite crystals covered with crystalline β-glucosidase are then

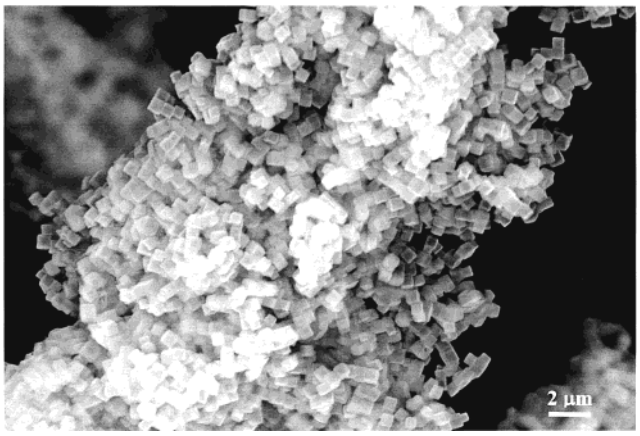

Figure 7. The aggregates of cubic zeolite-A crystals remaining after burning off the organic enzyme from the zeolite-A-β-glucosidase composite fiber.

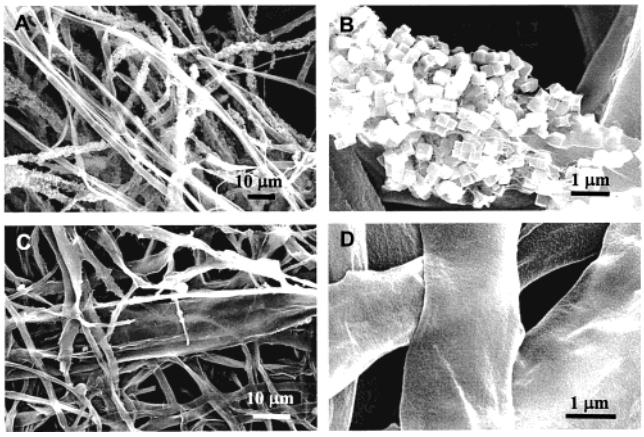

Figure 8. SEM images showing the fibers covered with unburied clusters of zeolite-A crystals on the external surface that resulted with the zeolite to enzyme weight ratio of 10 (A, B) and the smooth flat fibers that resulted with the corresponding ratio of 2.5 (C, D), at two different magnifications, respectively.

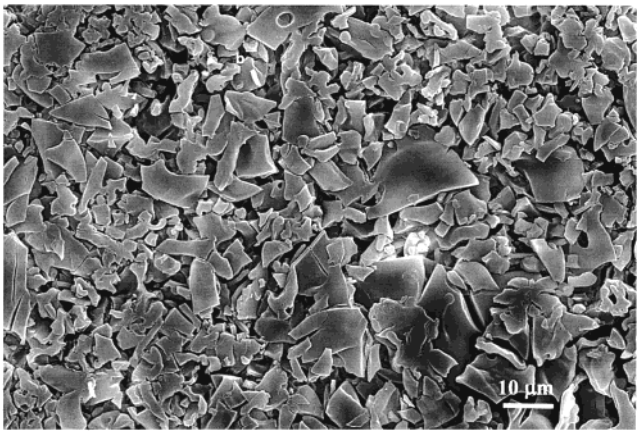

Figure 9. The SEM image showing the flat flakelike morphology of the crystalline β-glucosidase.

interconnected into clusters by further intergrown crystalline β-glucosidase (step C). We propose that continual crystallization of β-glucosidase between the zeolite clusters eventually leads to zeolite−enzyme composite fibers (step D). However, it remains to be elucidated why the organic−inorganic composite adopts this particular morphology. Nevertheless, it is certain that the entrapped zeolite crystals play crucial roles in shaping the overall structure of the composite fiber from the fact that

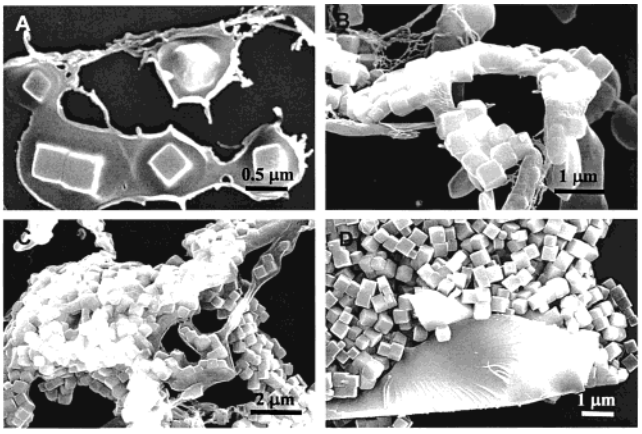

Figure 10. SEM images showing the initial and intermediate stages of the fibrillation process from a mixture of *β*-glucosidase and D-glucose-tethering zeolite-A in distilled deionized water (A, B, and C). Panel D represents that of a mixture of a pile of individual plain zeolite-A crystals and chunky crystalline *β*-glucosidase that results from phase separation of the turbid aqueous slurry of unmodified, plain zeolite-A crystals and *β*-glucosidase stirred for 24 h into its components upon drying.

rather flat fibers result upon increasing the relative amount of enzyme. The enzymes may transmit a recognition effect between the opposite faces of the zeolite crystals causing the growth process to be favored in an axial direction.

V. Enzymatic Activity of *β*-Glucosidase in the Fibrils. Interestingly, the light yellow strips of Reflectoquant immediately turned intense green upon dipping into the equilibrated solution of D-cellobiose and fibrils. This strongly indicates that D-cellobiose is hydrolyzed to D-glucose in the presence of the composite fiber. Consistent with the color test, the composite fiber also readily hydrolyzed PNPG into D-glucose and *p*-nitrophenol. The above results therefore clearly indicate that the enzymatic activity of *β*-glucosidase within the composite fiber is preserved. We propose that the enzymes existing in the periphery or at the outermost external surfaces of the fibrils provide the catalytic sites for the hydrolysis reactions. To our surprise, the enzymatic activity of the composite fibers persisted for more than 6 months even if they were kept in distilled deionized water at ambient temperatures. This indicates that the enzymes are very stable in the composite fiber as if they were stored in the crystalline state. This result raises the possibility to devise a novel method to preserve and immobilize the highly expensive enzyme on solid supports by modifying the procedures described in the Experimental Section.

Scheme 3

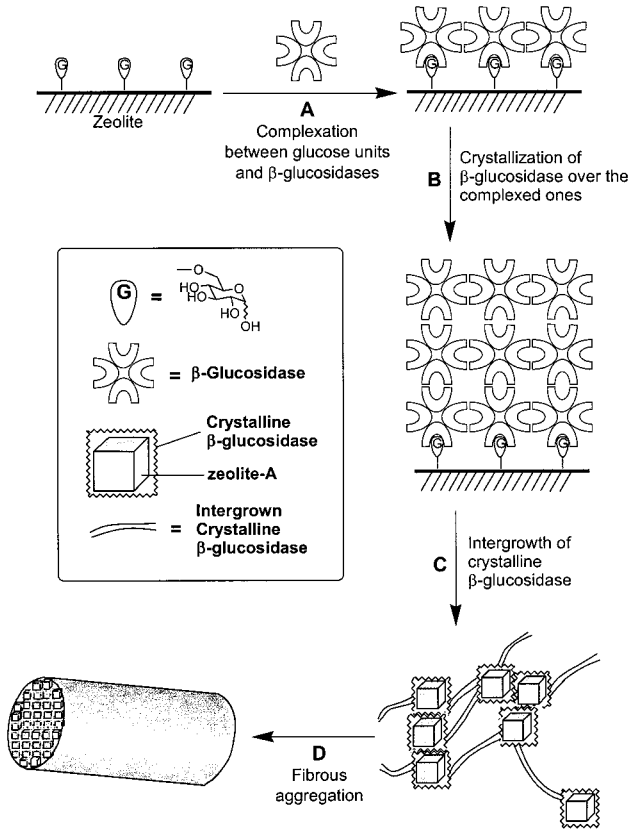

VI. Concluding Remarks. Overall, this report demonstrates for the first time the self-assembly of an enzyme and its substrate-tethering inorganic crystals into a fibrous composite material. This result opens the possibility that enzymes may serve as structure-forming agents in living organisms while retaining their enzymatic activities. From the fact that enzymes consist of proteins, the resulting material can be considered as a type of protein-inorganic composite material which plays a vital role in living organisms as structural material. This result also elucidates the remarkable behavior of *β*-glucosidase in the presence of the surface-bound D-glucose.

Acknowledgment. We thank the Ministry of Science and Technology (MOST), Korea, for supporting this work through the Creative Research Initiatives (CRI) program.

JA0028222